Commissioning of the ATLAS electromagnetic calorimeter with minimum bias events

F. Hubaut, P. Pralavorio

Centre de Physique des Particules de Marseille, CNRS/IN2P3 - Univ. Méditerranée, Marseille - France

ATL-LARG-PUB-2007-007

08 March 2007

Abstract

This note presents the potentiality to commission the ATLAS EM calorimeter during the (very) first days of data taking, prior to be able to trig and identify correctly electrons. For this purpose, a very simple analysis using the ϕ symmetry of the abundant minimum bias events and computing the energy accumulated in the EM calorimeter is proposed. No input from the Monte Carlo is necessary, and only information from the calorimeter is used. To cope with the high number of events, simulation and analysis are performed using the GRID technology. Adopting a simple energy reconstruction scheme based on the cosmic muon experience should allow to spot intrinsic problems of the EM calorimeter in a few days. It should also give first hints on the ϕ dispersion of the Inner Detector material, if the excess is sizeable $>10\%$ X_0 in a region $\Delta\eta \times \Delta\phi = 0.1 \times 0.1$. Ultimately, a first flavor of systematics coming from the EM calorimeter ϕ non-uniformity and its positionning (in the ATLAS framework or with respect to the beam) could be possible.

Contents

1 Introduction

Minimum bias events will give first and abundant proton-proton collision signals in LHC detectors, both at 900 GeV and at 14 TeV. They will constitute an interesting physics case to tune the Monte Carlo event generation [1]. They will also provide a tool to check *in situ* the behavior of the inner detector (ID) and the electromagnetic (EM) calorimeter. For the latter, this is especially interesting prior to be able to trig and identify correctly electrons from Z and W decays. Therefore, this note will concentrate on the results that can be obtained in the very first days of data taking (both at 900 GeV and at 14 TeV), relying only on the calorimeter data without any input from the Monte Carlo.

Only the region $|\eta| < 2.5$, devoted to precision physics in ATLAS (tracker coverage), will be considered in this note, excluding the zone around the barrel-endcap crack ($1.4 < |\eta| < 1.5$). As demonstrated with beam tests, the intrinsic performance of the EM calorimeter are well understood and reproduced by the simulation [2, 3, 4]. Especially, the response non-uniformity was measured to be less than 0.6% over complete module acceptance, $\Delta\phi = 2\pi/16(8)$ in barrel (endcap) [5]. It is therefore realistic to assume that the EM calorimeter will be uniform at 1% at the beginning of data taking, including possible *in situ* effects coming from temperature gradients in the cryostats or impurities in liquid argon. In this context, the purpose of this note is to assess how the ϕ symmetry of minimum bias event activity can be a useful probe to spot problems: any distortion of this symmetry may come from the matter in front of the calorimeter, from the EM calorimeter itself (dead channels, HV problems), from its position in the ATLAS framework or with respect to the beam (transverse position or collision angle).

The note is organised as follows. Characteristics of minimum bias events, detector geometry and simulation tools are described in section 2. A brief description of the EM calorimeter and the energy reconstruction scheme is given in section 3. Sensitivities to EM calorimeter and ID matter obtained with minimum bias events are then presented in section 4. Finally, section 5 is dedicated to conclusions.

2 Full simulation of minimum bias events

This section starts with a brief overview of minimum bias event characteristics (section 2.1), and then describes the specific ATLAS geometry used in the following (section 2.2). Finally, this study requires the full simulation of several hundred thousands events, which represents a technical challenge in terms of time and data size, briefly reviewed in section 2.3.

2.1 General minimum bias event characteristics

Minimum bias events are associated with inelastic proton-proton collisions. Most of the activity in the central region of the detector ($|\eta| < 2.5$) will be due to non-diffractive events and, to a much less extent, to double diffractive events. The associated cross-section is around 50 ± 1 mb at 900 GeV from UA5 measurements [6] and is extrapolated to 70 mb at 14 TeV [1], with an uncertainty above 10%. The average transverse energy produced per event is almost flat up to

$|\eta| = 2$ and then rises with $|\eta|$ [7]. It is carried from the primary vertex toward the calorimeter by a few hundreds of low energy photons ($\sim 50\%$) and charged pions ($\sim 40\%$) with a p_T peak ~ 250 MeV [8]. This composition is similar at 900 GeV, with a multiplicity reduced by 40% and even smaller p_T. As charged pions are deflected by the magnetic field, most of them will not reach the calorimeter (typically those with $p_T < 500$ MeV). It is also the case for half of photons converting in the ID. Therefore most of the energy deposited in the EM calorimeter will come from photons that did not convert in the ID.

The sum of transverse energies deposited in all the EM calorimeter cells is in average 20 GeV for 14 TeV collisions [7]. Because of this small amount of energy deposited per event, spread over the full calorimeter coverage, it is more interesting to think in terms of energy flow. Assuming a large number of events, O(10^6), this energy flow is symmetric in ϕ, i.e the accumulated transverse energy is the same for all EM calorimeter cells in a given η ring.

2.2 ATLAS detector simulation

For the EM calorimeter, the accumulation of minimum bias events can be seen as a photon energy flow symmetric in ϕ. Assuming an ideal (no dead channels or HV failures) and perfectly uniform detector, any distortion of this symmetry could come from a non-uniform ϕ matter distribution before the active part of the EM calorimeter or an imperfect positionning of the calorimeter in the ATLAS framework. To quantify the sensitivity to such effects, a distorted and misaligned geometry of the ATLAS detector, called CSC-01-02-00 [9], is used.

To obtain a distorted geometry, the idea is to start from present estimations of material[1] in the inner detector and in front of the EM Calorimeter, coming from precise weighting measurements and testbeam results. A realistic amount of additional material, that may come from cable routing or underestimation of material budget, is then inserted at a given η in one ϕ hemisphere. For the ID, the choosen region is $0 < \phi < \pi$. Figure 1 (left) shows the η distribution of the ID material in terms of radiation lenght (X_0) for the two different ϕ hemispheres. The additionnal material varies in η between 0.05 and 0.6 X_0. A similar situation occurs for the matter in front of the barrel EM Calorimeter, but in the region $-\pi/2 < \phi < \pi/2$ as illustrated in Figure 1 (right). Figure 2 shows these relative excess as a function of η for the inner detector (left) and for the material in front of the EM calorimeter (right).

The position of the barrel and endcap EM calorimeters in the ATLAS framework will be checked *in situ* with physics data after geometrical surveys, and will be only partly probed with cosmic muons. Misalignments may come from a combination of detector deformations, cryostat rotations and translations around the beam axis or the vertical axis. A tentative was made to implement these last two effects in the geometry, as illustrated in Figure 3. It affects mostly the endcaps: *i*) an horizontal displacement of 4 cm away from the interaction point alters the projectivity along η, resulting in a misalignment up to half a cell; *ii*) this misalignment depends on ϕ, with a peak-peak amplitude of $1/2$ ($1/4$) of one cell in endcap C (A).

[1] As minimum bias events are mainly composed of low energy photons in the EM calorimeter, the most relevant information is the number of radiation lenghts crossed by the particles.

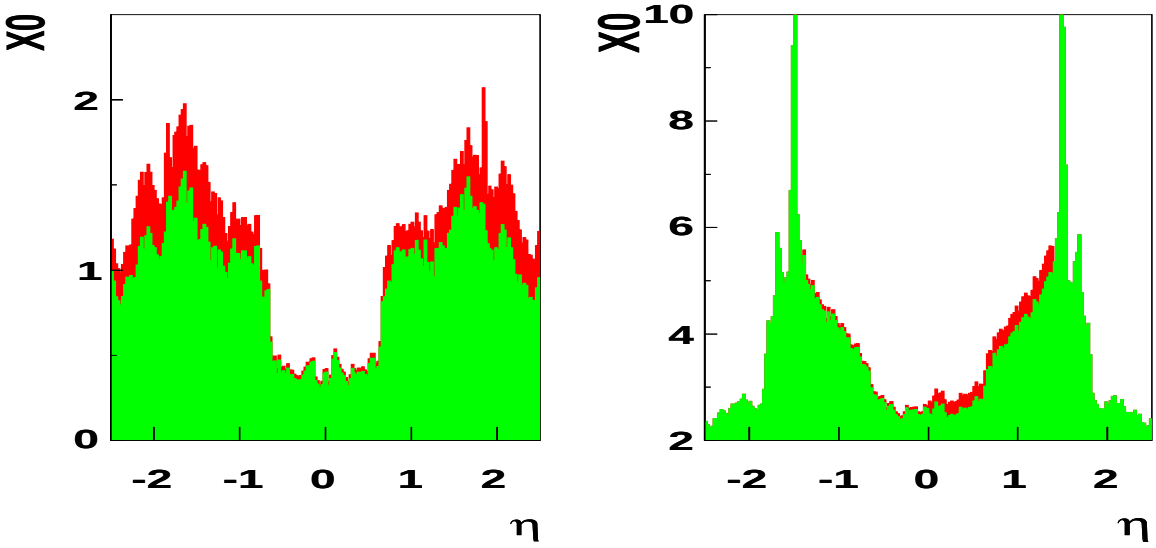

Figure 1: *Number of radiation lenghts, X_0, as a function of* h, *in the inner detector (left) and in front of the EM Calorimeter (right) with CSC-01-02-00 geometry. Green represents the nominal values. Red represents the distorted values in the hemisphere* $0 < f < p$ *(left) and* $-p/2 < f < p/2$ *(right).*

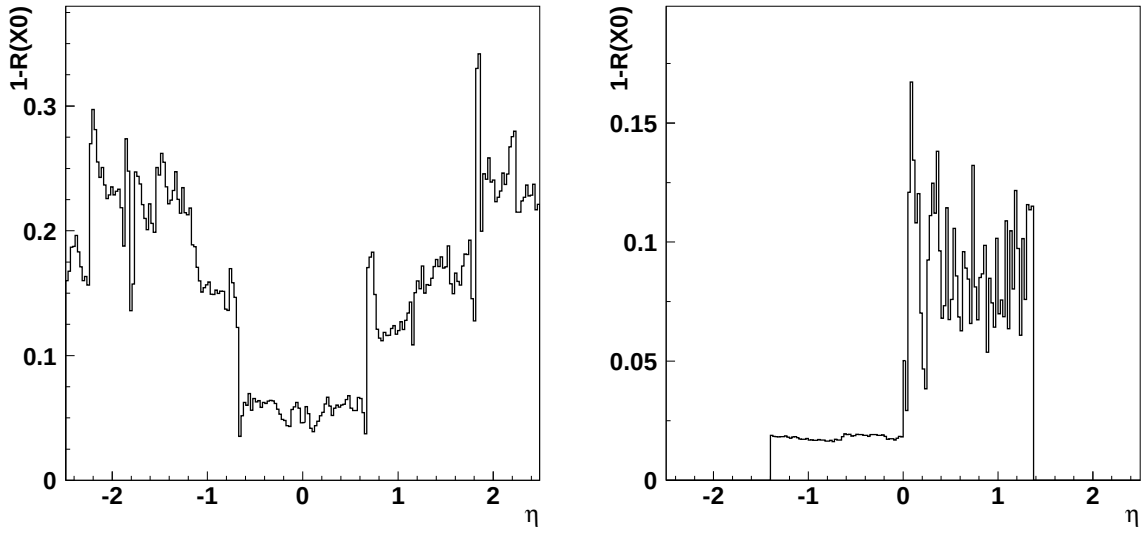

Figure 2: *Relative increase of number of radiation lenghts, $R(X_0) = DX_0/X_0$, in the distorted hemispheres, injected in CSC-01-02-00 geometry in the inner detector (left) and in front of the EM calorimeter (right), as a function of* h *(see Figure 1).*

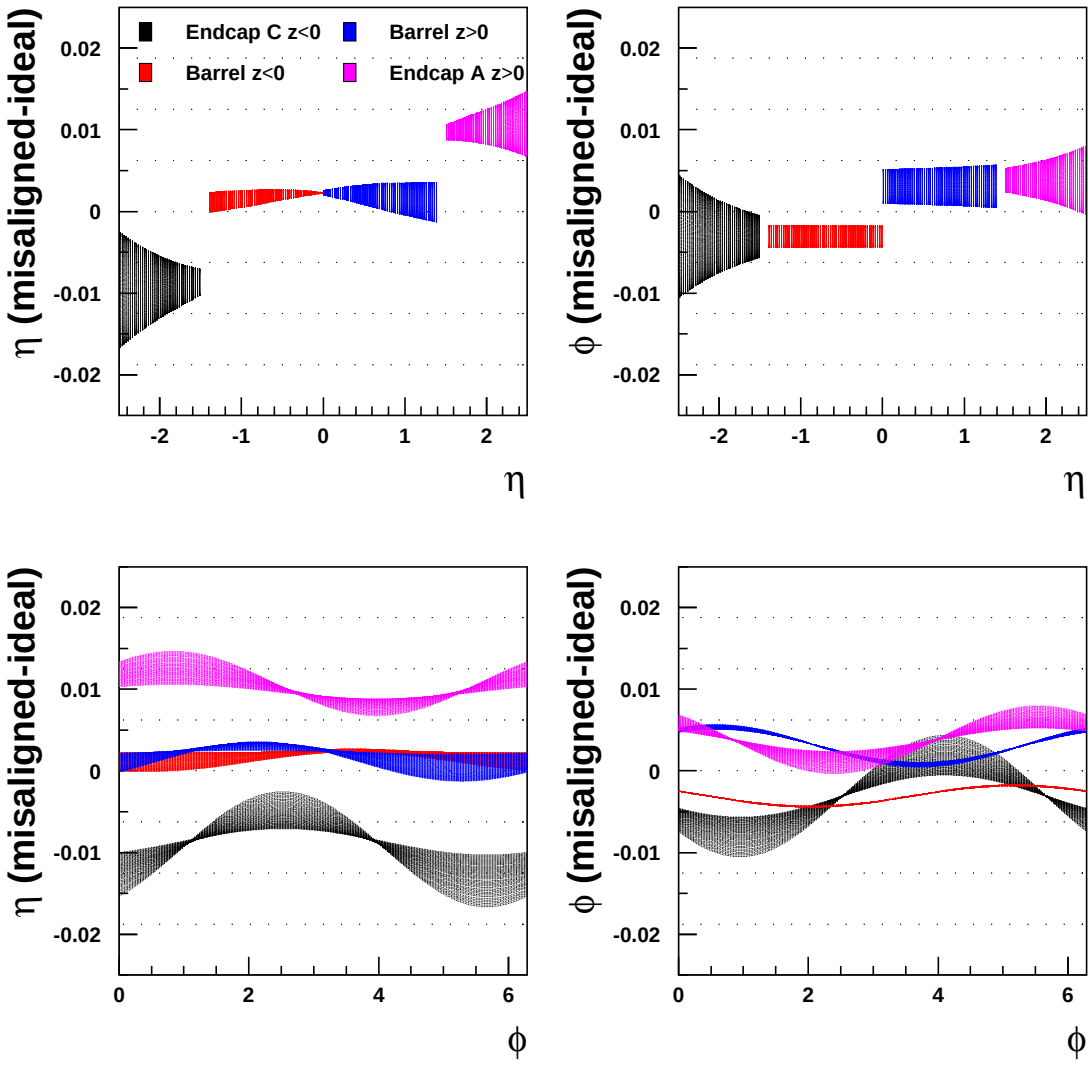

Figure 3: *Misalignments* Dh *(left) and* Df *(right) of the EM Calorimeter introduced in CSC-01-02-00 geometry with respect to its ideal position, as a function of* h *(top) and* f *(bottom). Horizontal dotted lines indicates 1/4th of a cell size.*

2.3 Full event simulation on the GRID

Simulating a large number of events with a detailed description of the detector is a technical challenge. In this note, we restrict ourselves to the 500 000 (100 000) inelastic non-diffractive events at 14 (0.9) TeV generated by ATLAS for the last data challenge before the LHC start-up, called CSC [2]. Single and double diffractive events (sample 5002) are not used, which should not change our conclusions as their contribution to the energy deposit in the central part of the calorimeter is very low. No pile up has been added, which is negligible at the beginning of data taking when this study is of interest. The modelling of underlying event and generator choice (Pythia [10] vs Phojet [11]) should also have no impact on our analysis.

In average, GEANT4 [12] deals with 17 500 tracks with $E > 50$ MeV per event. An effort was made to optimize the simulation+digitization process by keeping only the ID and the calorimeters. Each event simulation takes around 600 s CPU time. Using the GRID technology to parrallelize the load, it is possible to reach 1 s, i.e. around one week (day) for 500 000 (100 000) events at 14 (0.9) TeV [13]. Because of $\sim$ 15% of failures due to GRID problems, only 418 250 (86 500) events at 14 TeV (0.9) TeV were simulated and digitized with ATHENA version 12.0.3. Finally, only the energy accumulated in all EM calorimeter cells is recorded in a slimmed ESD (200 kBytes per event). This last step, mimicking the raw data processing, takes 2 s per event.

Despite this effort, the simulated sample corresponds roughly to $1/10^{\text{th}}$ of the statistics foreseen per day (see section 4.1). It is worth to notice that this limitation in the simulated statistics will not be a problem for real data analysis, as the latter will not rely at all on the Monte Carlo.

[2] The corresponding samples are csc11.005001.pythia_minbias.evgen.EVNT.v11004202 and csc11.005005.pythia_minbias_900.evgen.EVNT.v11004208.

3 EM calorimeter energy reconstruction for minimum bias events

In this section, a presentation of the EM calorimeter energy reconstruction scheme adapted to minimum bias events is presented, insisting on the difference with the usual analysis performed for electrons.

3.1 Detector granularity

In the ATLAS precision region ($|\eta| < 2.5$), excluding the zone between the barrel-endcap crack ($1.4 < |\eta| < 1.5$), the EM calorimeter is divided in depth in three projective compartments of lenght 4, 16-18 and 4-12 X_0, for the first (S1), second (S2) and third (S3) sampling, respectively[3]. It is segmented in a total of about 170 000 read-out channels, as reminded in Table 1. The High Voltage (HV) is distributed in $\Delta\eta \times \Delta\phi = 0.2 \times 0.2$ regions[4]. The two sides of the electrodes are supplied by different HV cables.

Optimizing the signal to noise ratio is crucial to measure the low energy flow from minimum bias events. S2 cells of size $\Delta\eta \times \Delta\phi = 0.025 \times 0.025$ can be used, as well as a combination of S1 and S2 cells. In this case, the minimum tower of S1 and S2 cells has a larger size $\Delta\eta \times \Delta\phi = 0.025 \times 0.1$, as sketched in Figure 4.

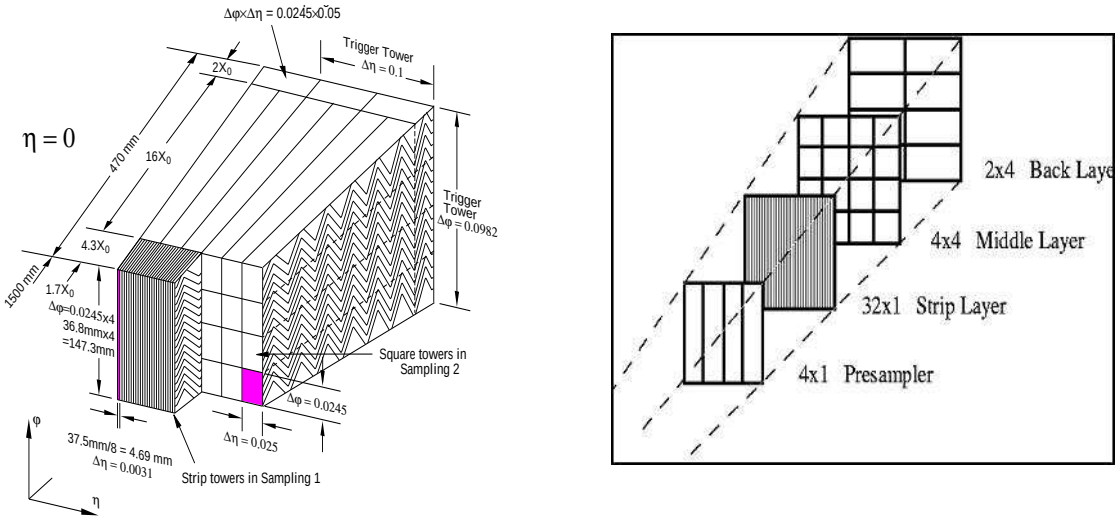

Figure 4: *Sketches of a $\Delta\eta \times \Delta\phi = 0.1 \times 0.1$ region of the EM calorimeter with the different layers in depth. In the endcaps, the number of strips can be 32, 24, 16 or 4 (Table 1).*

[3] A thin presampler (PS) detector of 0.1 X_0 is present for $|\eta| < 1.8$.

[4] In the endcaps, some regions are of size $\Delta\eta = 0.1$

Region	Compartments ($\Delta\eta \times \Delta\phi$)			
	PS (0.025×0.1)	S1 ($0.025/n^*\times0.1$)	S2 (0.025×0.025)	S3 (0.050×0.025)
Barrel	112×64	896×64	112×256	54×256
Endcaps	24×64	424×64	80×256	40×256
Total	8704	84480	49152	24064

Table 1: *Number of cells ($\eta \times \phi$) in the precision region of the EM calorimeter, $|\eta|<2.5$, without the zone $1.4<|\eta|<1.5$ around the crack. *n=1, 4, 6, 8, depending on η.*

3.2 Energy reconstruction scheme

A coherent scheme for the electron energy reconstruction in ATLAS has been developped and debugged during intensive beam test programs [3]. The main ingredients are a very accurate calibration scheme for the read-out electronics, a signal reconstruction based on an optimal filtering technique [14], allowing to minimize the noise contribution, and a ponderation of corrected energies measured in the different compartments. This scheme has been proven to optimize both detector linearity and energy resolution [3].

This energy reconstruction procedure is partially included in the ATLAS simulation, but this level of details is not suited here. This is mainly due to the energy range (typically tens of GeV for electrons and hundreds of MeV for minimum bias, closer to the noise level) and the absence of clusterisation for the measurement of the energy flow. For all these points, the approach adopted in the present note is similar to the one used for cosmic muon analysis [15, 16] and may therefore benefit from its developements, especially to improve the signal to noise ratio. As an exemple, using 29 samples instead of the usual 5 for the energy reconstruction lowers the noise level by a factor 2 [17]. From this point of view, all results obtained in the following are conservative, as the signal extraction is only related to the noise level. On the other hand, it is assumed that the noise is well under control, especially that it does not depend on the time or on the front end crate.

3.3 Reconstruction of minimum bias events energy flow

Figures 5 and 6 show the response to 420000 minimum bias events of a typical cell for each layer of the barrel and endcap EM calorimeter. Such a statistics should be available very quickly, both at 900 GeV and 14 TeV (section 4.1). The noise value, extracted from testbeam results [2], is typically 30 MeV for S2 cells and 15 MeV for S1 cells (see discussion for possible improvement in section 3.2). Above the noise, a clear signal tail is visible in each compartment of the calorimeter and should allow to determine the problematic cells (section 4.2). Table 2 quantifies these tails by indicating the number of events above 5 σ for 420000 initial events. At 14 TeV, the occupancy in all cells is greater than several tens, far above the expected noise contribution. To obtain similar results with 900 GeV data, we can estimate from Table 2 that a 3 to 5 times greater statistics will be necessary. The results in the following will be shown for 14 TeV proton-proton collisions.

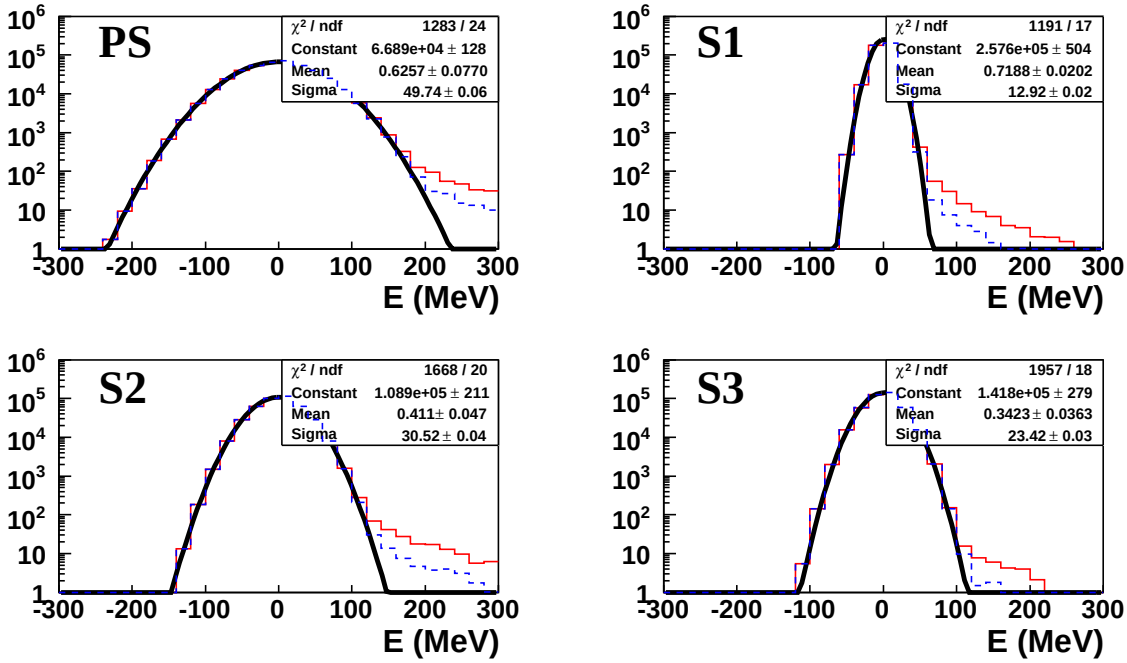

Figure 5: *Typical energy distributions in one barrel cell of each compartment for* 420 000 *events. Full (dashed) histograms are obtained at 14 TeV (900 GeV). Gaussian fits to the noise contribution are superimposed.*

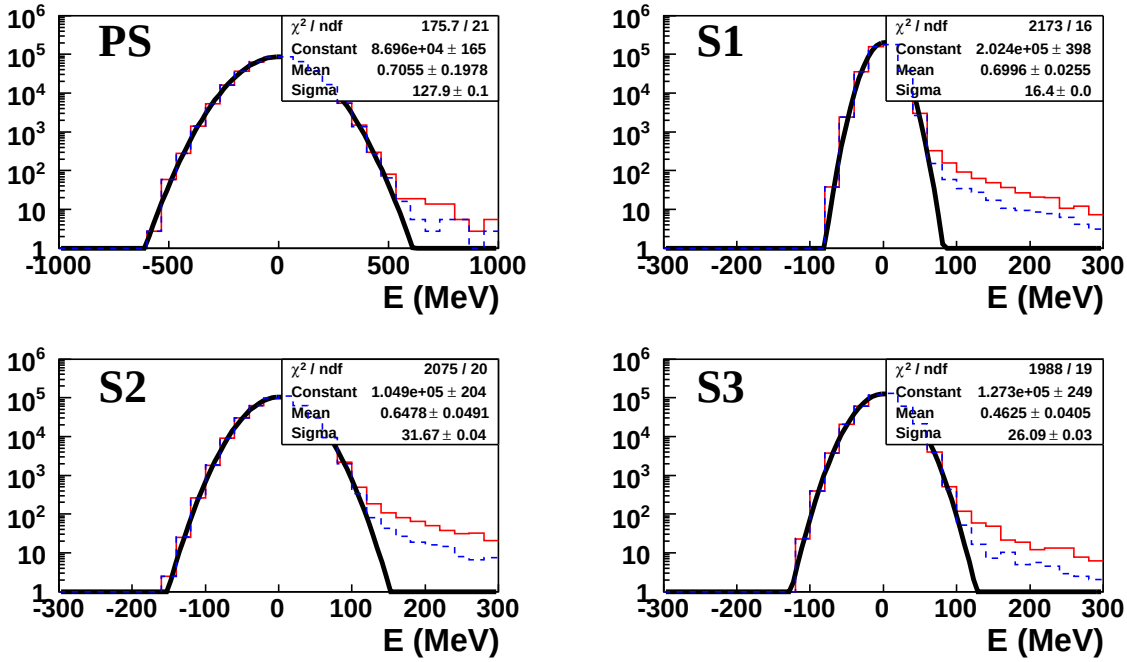

Figure 6: *Typical energy distributions in one endcap cell of each compartment for* 420 000 *events. Full (dashed) histograms are obtained at 14 TeV (900 GeV). Gaussian fits to the noise contribution are superimposed.*

The energy in the cells is accumulated over all the events if its value is 5σ above the noise (see Figures 5 and 6). An upper cut to supress fluctuations due to high energy deposits is not useful with our available statistics of several hundred thousands events. The error on the accumulated energy is computed as described in Appendix 1. It is worth noticing that this analysis, performed on the ESD Cell calo container, takes one hour using the GRID technology.

Calorimeter	Barrel				Endcap			
Cell type	PS	S1	S2	S3	PS	S1	S2	S3
Events above 5σ (14 TeV)	270	120	150	30	80	570	490	210
Events above 5σ (900 GeV)	90	30	40	10	20	220	150	60

Table 2: *Number of events per cell of each compartment with an energy deposit 5σ above the noise for* 420 000 *minimum bias events, as extracted from Figures 5 and 6. Expected number of events from the noise Gaussian tail is 0.1.*

4 Commissioning with minimum bias events

Minimum bias events will allow to have a first and quick look at the entire EM calorimeter, spotting intrinsic problems (section 4.2) and giving first quantitative hints on the ID material dispersion in ϕ (section 4.3). They could also help to address more subtle problems of the EM calorimeter (section 4.4), probably less relevant when it will be possible to trig and identify correctly electrons from Z and W decays. The present study is limited by the available Monte Carlo statistics. It is illustrates what could be done with real data, which will not rely at all on the Monte Carlo.

4.1 Triggering issues

The huge cross-section will allow to record lots of minimum bias events in the early running. Even with a low luminosity of 10^{29} cm^{-2} s^{-1}, the bandwidth will be trigger-limited. A dedicated device based on scintillation counters has been installed in the endcap region, $2.1 < |\eta| < 3.8$, in front of the calorimeter cryostats for triggering purpose in the early running [18]. This will be mainly dedicated to physics studies of minimum bias events themselves. To commission the EM calorimeter, a more suited approach would be to trig on random bunch crossings where the number of minimum bias events would be around 10% at early stage of collisions [19]. If a 1 kHz L1 bandwidth would be dedicated, $\sim$ 100 Hz could be selected at the HLT level or offline. With a 30% efficiency, this would result in 3 millions of events per day.

4.2 Detecting EM calorimeter HV and signal problems

The EM calorimeter has been extensively tested, allowing to establish a detailed map of the few HV and signal problems [20]. As an example, $\sim 0.02\%$ of the channels are dead (no signal in calibration) and HV problems affect only a few percents of the full coverage. As the simulation assumes a perfect detector response (*i.e.* no dead channels or HV failures), these two kinds of problems have been introduced at the analysis level.

Minimum bias events will firstly allow to detect dead cells in the electromagnetic calorimeter. As experienced during beam tests, some cells can de dead (no signal in physics) with a good response to calibration pulses. This could be seen with cosmic muons, but not on the entire calorimeter coverage. Figure 7 (left) shows how a dead middle cell could be seen with 420 000 events. A map of all dead cells could be available in a few days for all layers of the barrel and endcap EM calorimeter, as tails at high energy above the noise are clearly seen for all the cells (Table 2).

Other kind of problems, such as HV failures, can also be probed. As an example, in the case of an unknown HV failure on one sector size, the energy would be divided by 2. This would be clearly seen on the accumulated energy as a function of f. This is illustrated in Figure 7 (center) for the barrel case at low h (most difficult case) with 420 000 events. The case where one electrode only is faulty, shown in Figure 7 (right), will require more statistics.

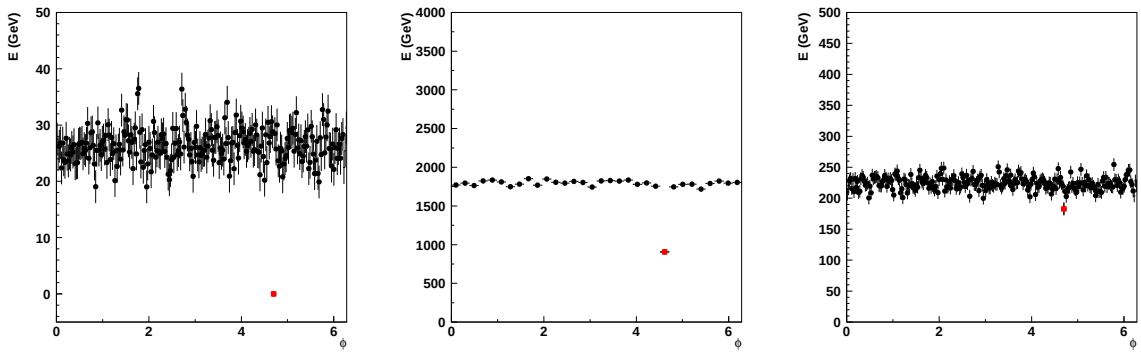

Figure 7: *Energy accumulated for* 420 000 *events at 14 TeV, as a function of* f *in different regions of the EM Calorimeter. Left: in each S2 cell at* $\mathsf{h} = 0.2$*; Center: in each HV sector at* $0.2 < \mathsf{h} < 0.4$*; Right: in each S2 cell at* $0.2 < \mathsf{h} < 0.4$*. Injected problems are indicated with a red square. Left: Dead S2 cell; Center: All electrodes of one HV sector fed on one side only; Right: One electrode used to form a S2 cell fed on one side only.*

4.3 Sensitivity to inner detector material

As detailed in section 2.2, a ϕ asymmetry in the ID matter distribution has been introduced in the simulated geometry, with an increase in hemisphere $[0,\pi]$ (Figures 1 and 2). As already discussed in section 2.1, most of the particles reaching the EM calorimeter are low energy photons that did not interact with the inner detector material. Therefore, in a given $\Delta\eta$ zone, the presence of a dip along ϕ in the accumulated energy can reveal the presence of unexpected material.

To evaluate the sensitivity to this effect with the available statistics, zones of $\Delta\eta = 0.1$ are considered. Figure 8 shows the accumulated transverse energy in four of these regions, as a function of ϕ. A step at $\phi = \pi$ is visible where the change in ID matter is large enough. This effect is illustrated for the $-2.0 < \eta < -1.9$ region in Figure 9, which shows the top left plot of Figure 8 projected on the energy axis for both hemispheres, $0 < \phi < \pi$ (top) and $\pi < \phi < 2\pi$ (bottom). The mean transverse energy is significantly different between both hemispheres, and the ratio

$$R(S2) = \frac{< E_T^{S_2}(\pi < \phi < 2\pi) >}{< E_T^{S_2}(0 < \phi < \pi) >} \tag{1}$$

is equal to 1.117 ± 0.005. The presence of 23% more ID material in the $0 < \phi < \pi$ hemisphere for $-2.0 < \eta < -1.9$ reduces significantly the energy deposited in the EM calorimeter.

The correlation between the ID matter excess and $R(S2)$ is shown in Figure 10 for all $\Delta\eta = 0.1$ regions of the calorimeter. This gives a quantitative illustration of the $R(S2)$ sensitivity to an excess of ID matter greater than 10%. Using the parametrization shown on Figure 10, it is possible to extrapolate to a more realistic situation, by varying the size of the $\Delta\eta \times \Delta\phi$ window representing the size of the ID matter excess. Assuming no systematic effects, the number of events needed to see a 5σ effect in a given $\Delta\eta \times \Delta\phi$ window can be read from Figure 11 (see Appendix 1 for details about the computation). As an example, with 3 millions of events (~ 1 day), it is possible to identify a region $\Delta\eta \times \Delta\phi = 0.2 \times 0.1$ with a 15% X_0 ID matter excess.

The results quoted in Figure 11 should be taken with care, as they assume no systematic effects. As mentionned in section 2.2, a possible effect can come from the absolute positionning of the calorimeter in the ATLAS framework, whose maximal deviation from ideal position will be reached in the endcaps. This explains the slight systematic shift observed in Figure 10 for the two endcaps. The ϕ dependence of the η distortion (Figure 3, bottom left) associated with the small variation of the transverse energy deposited along η can lead to a slight distortion of the energy deposition along ϕ. This is illustrated in Figure 12 at $\eta = -2.3$, where the effect is maximal. A similar behaviour would be observed in case of a vertical displacement of the beam or a shift of the collision angle. Other systematics can come from the variation with ϕ of the matter quantity just in front of the calorimeter, but the available statistics was not enough to come to a quantitative conclusion on this point.

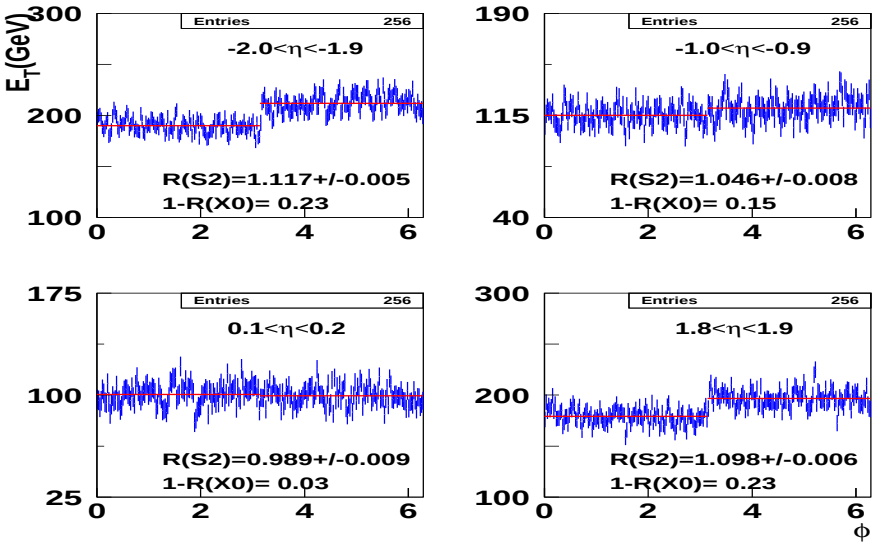

Figure 8: *Accumulated transverse energy in S2 cells, as a function of* f*, in four* $\mathsf{Dh} = 0.1$ *regions with different ID matter excess 1-R(X0) in the hemisphere* $0 < \mathsf{f} < \mathsf{p}$*. This is obtained with* 420 000 *minimum bias events at 14 TeV. The top left histogram is projected on the y axis in Figure 9.*

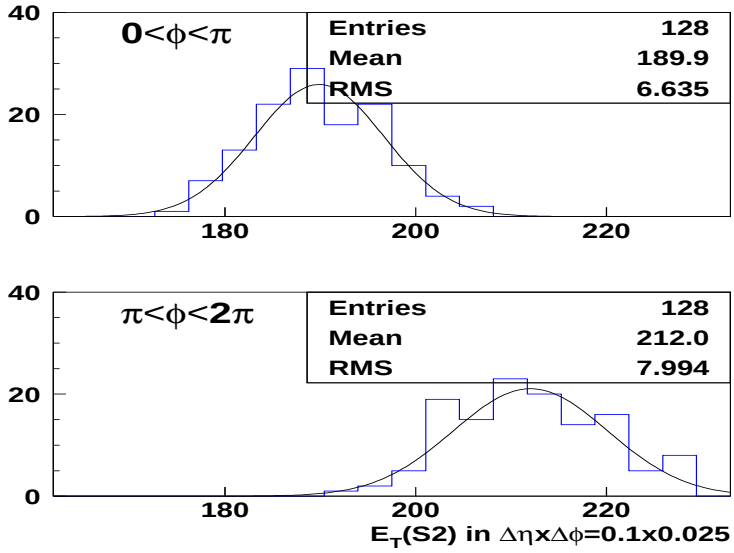

Figure 9: *Distribution of the transverse energy accumulated in the 128* $\mathsf{Dh} \times \mathsf{Df} = 0.1 \times 0.025$ *S2 regions of both hemispheres,* $0 < \mathsf{f} < \mathsf{p}$ *(top) and* $\mathsf{p} < \mathsf{f} < 2\mathsf{p}$ *(bottom). This is obtained for* $-2.0 < \mathsf{h} < -1.9$ *with* 420 000 *minimum bias events at 14 TeV. Gaussian fits are superimposed.*

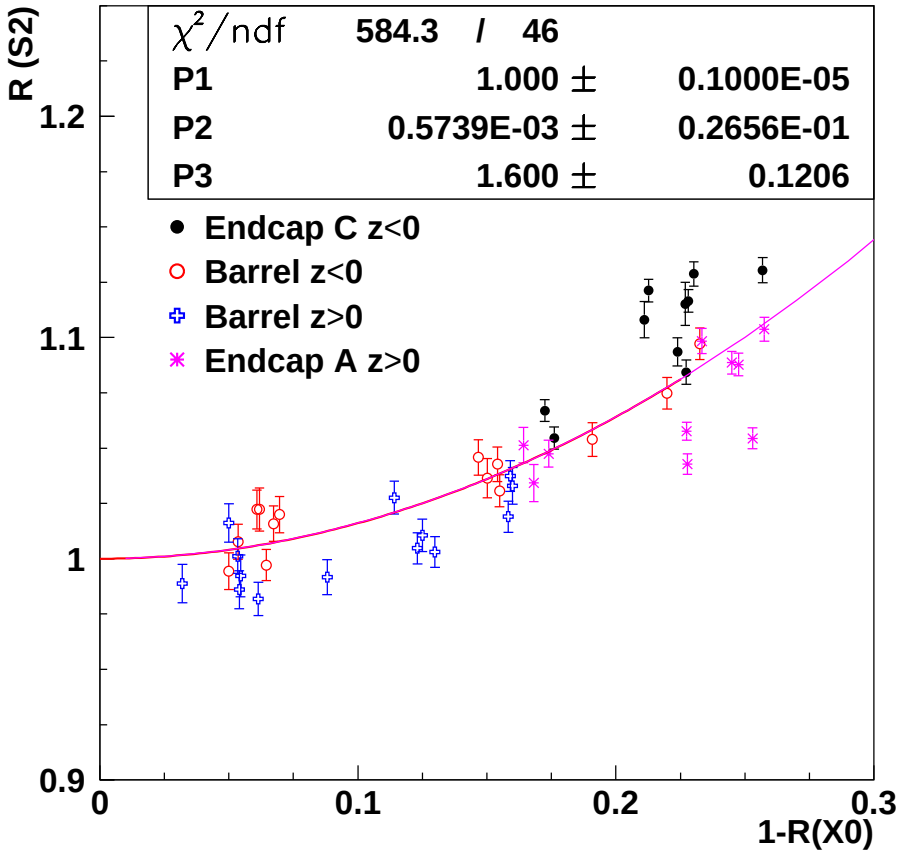

Figure 10: *R(S2), ratio of accumulated transverse energy in S2 between the hemispheres* $0 < \mathsf{f} < \mathsf{p}$ *and* $\mathsf{p} < \mathsf{f} < 2\mathsf{p}$ *(see Equation (1)), as a function of the ID matter excess, 1-R(X0) (see Figure 2 (left)), for all* $\mathsf{Dh} = 0.1$ *regions. The location (endcap or barrel,* $z > 0$ *or* $z < 0$*) of each region is indicated. A quadratic fit is superimposed.*

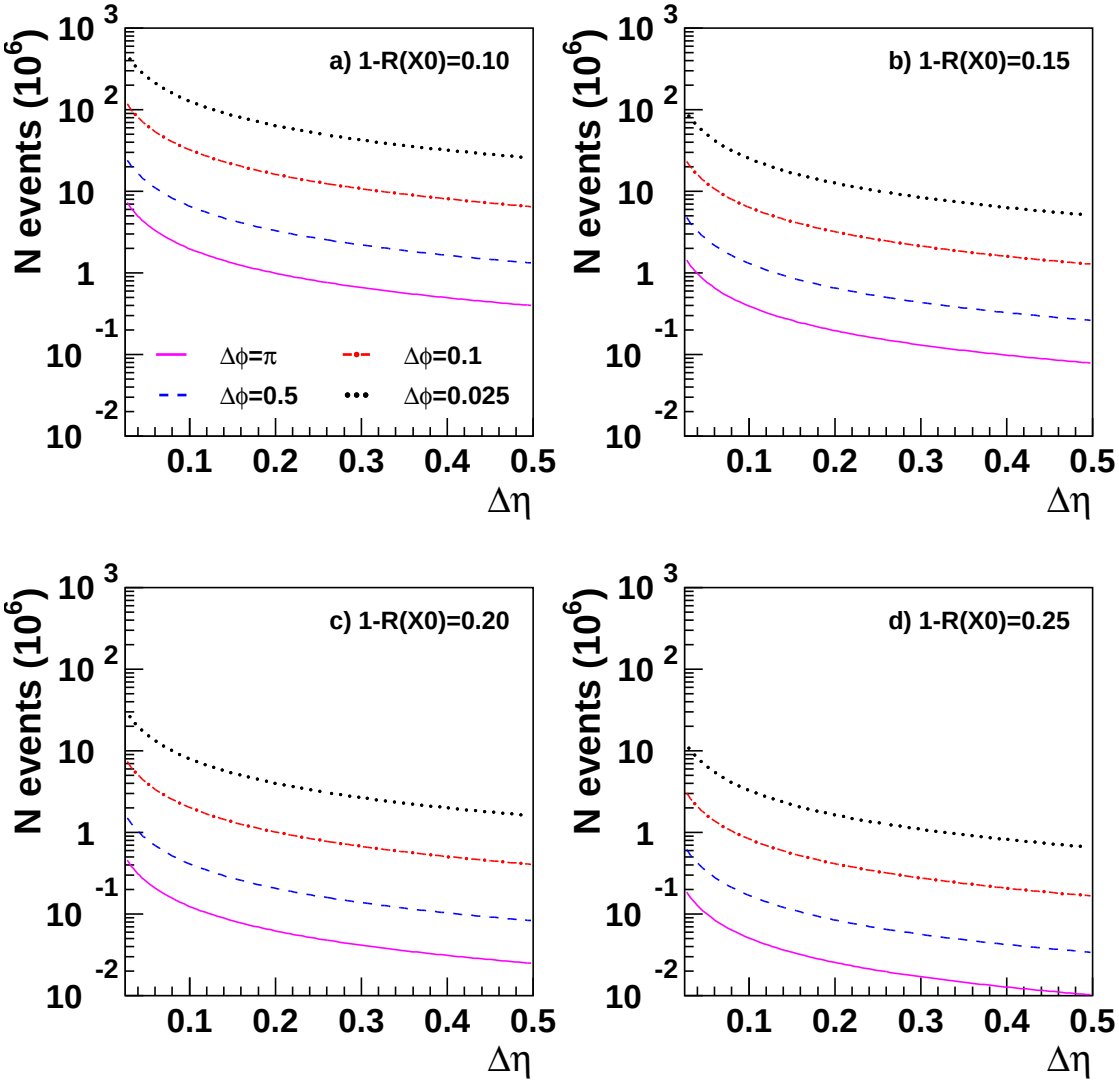

Figure 11: *Number of minimum bias events needed to see a* 5s *effect in the* f *symmetry of the energy deposit coming from an ID matter excess* $1 - R(X_0)$. *An excess of a) 10%, b) 15%, c) 20% and d) 25% is assumed to affect a* Dh × Df *zone. Results are based on a pure statistical extrapolation.*

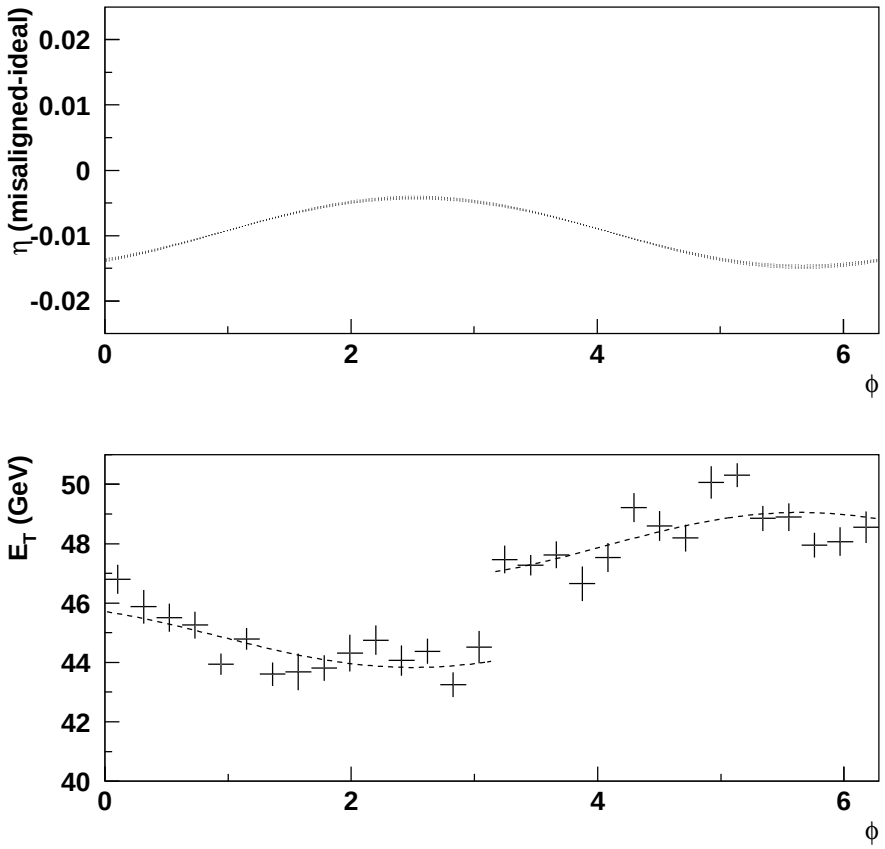

Figure 12: *Illustration of the correlation between the calorimeter misalignment (*$\Delta\eta$ *as a function of* ϕ *on the top plot, extracted from Figure 3), and the* ϕ*-dependence of the transverse energy accumulated in S2 cells (bottom plot). These results have been obtained at* $\eta = 2.3$ *with* 420 000 *minimum bias events at 14 TeV. The dashed line (bottom) is the result of a cosine fit, whose phase is extracted from the upper plot. The step at* $\phi = \pi$ *is due to the increase of ID material injected in CSC-01-02-00 geometry.*

4.4 Hint on EM calorimeter non-uniformity along f

The EM calorimeter should be uniform at 1% at the beginning of data taking. If systematic effects are under control, f-uniformity may be possible to check using minimum bias events. The ID matter sensitivity of the transverse energy accumulated in S2-cells, shown in Figure 10, is probably an obstacle. In this context, the ratio of transverse energy deposited in S1 and S2, with a coarser f granularity $\Delta f = 0.1$, is probably a better solution:

$$R(S1/S2) = \frac{< E_T^{S_1}(p < f < 2p) > / < E_T^{S_2}(p < f < 2p) >}{< E_T^{S_1}(0 < f < p) > / < E_T^{S_2}(0 < f < p) >} \quad (2)$$

Figure 13 illustrates that this variable has no dependence at first order with the ID matter excess, contrarily to $R(S2)$ (Figure 10). The statistical precision that can be reached on the $S1/S2$ variable uniformity along f lies between 3% (endcaps) and 11% (barrel) with 420 000 events at 14 TeV. Assuming no systematic effects, this could be extrapolated to a 2% level with ten millions of events, i.e. in few days. The main systematics will probably come from the knowledge of matter just in front of the EM calorimeter. However, the available Monte Carlo statistics is too poor to come to a more robust conclusion. This result can not be easily transposed to the electron case, but can be complementary because of the absence of clustering in the minimum bias approach.

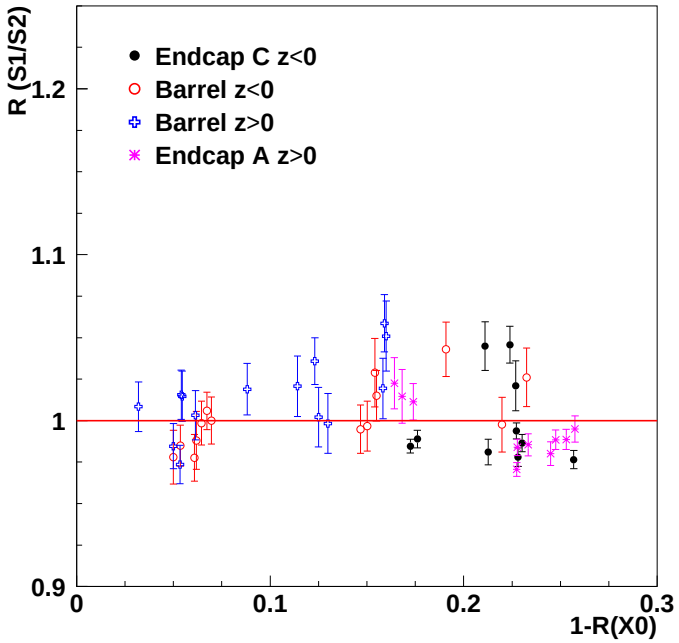

Figure 13: *R(S1/S2), as defined in Equation (2), as a function of the ID matter excess, 1-R(X0), for all* $\Delta h = 0.1$ *regions. The location (endcap or barrel,* $z > 0$ *or* $z < 0$*) of each region is indicated.*

5 Conclusions

Minimum bias events will give first and abundant proton-proton collision signals in LHC detectors, both at 900 GeV and at 14 TeV. Analysing these events with the foreseen ATLAS software facilities (including the GRID technologies) is a good exercise to get prepared for the first data. They will provide a good opportunity to commission the EM calorimeter in the ATLAS environnement with physics data, prior to be able to trig and identify correctly electrons from Z and W decays.

Using the ϕ symmetry of the minimum bias events and assuming a non-uniformity below 1% for the EM calorimeter (thanks to the test beam results), it is possible to perform a simple energy flow analysis based on the EM calorimeter data only. The results of this analysis are partly limited by the available statistics of fully simulated events, despite an important effort to optimize both CPU and space consumptions. It establishes that a complete mapping of the HV and signal problems for the EM calorimter could be drawn in a few days, and that major problems in the inner detector material description (excess of more than 10% of X_0) could be detected. Further effects like absolute positionning of the EM calorimeter in the ATLAS framework or a few percents ϕ non-uniformity of its response can then start to be addressed. This will be less relevant as soon as it will be possible to extract a clean electron sample from Z and W decays, which will allow finer studies.

References

[1] A. Moraes, C. Buttar and I. Dawson, *Prediction for minimum bias and the underlying event at LHC energies*, SN-ATLAS-2006-057.
Comparison of predictions for minimum bias event generators and consequences for ATLAS radiation background, ATL-PHYS-2003-020.

[2] B. Aubert *et al.*, *Performance of the ATLAS Electromagnetic Calorimeter Endcap Module 0*, Nucl. Instr. Methods A**500** (2003), 178.

B. Aubert *et al.*, *Performance of the ATLAS Electromagnetic Calorimeter Barrel Module 0*, Nucl. Instr. Methods A**500** (2003), 202.

[3] M. Aharrouche *et al.*, *Energy linearity and resolution of the ATLAS Electromagnetic Barrel calorimeter in an electron test beam*, submitted to Nucl. Instrum. Methods A, physics/0608012.

[4] J. Colas *et al.*, *Position resolution and particle identification with the ATLAS EM Calorimeter*, Nucl. Instr. Methods A**550** (2005), 96.

[5] F. Hubaut and C. Serfon, *Response uniformity of the ATLAS electromagnetic endcap calorimeter*, ATL-LARG-2004-015.

M. Kado, *Uniformity of LAr EM barrel and endcap modules*, presentation at LARG Week Plenary Meeting, Dec. 2006.

[6] UA5 Collaboration, *Antiproton-proton cross sections at 200 and 900 GeV cm energy*, Z. Phys. **C** 32 (1986) 153.

[7] A. Trzupek, *Transverse energy (E_T) in Minimum Bias pp events*, presentation at MinBias Working Group Meeting, Oct. 2006.

[8] D. Damazio, *MinBias events in 11.0.42*, presentation at MinBias Working Group Meeting, Aug. 2006.

[9] https://twiki.cern.ch/twiki//bin/view/Atlas/DistortedMaterial

[10] T. Sjöstrand *et al.*, *Pythia 6.3: Physics and Manual*, FERMILAB-PUB-03-457, LU-TP-03-38, hep-ph/0308153 .

[11] R. Engel, *Photoproduction within the two component dual parton model. 1. Amplitudes and cross-sections.*, Z Phys. C**66** (1995) 203.

[12] S. Agostinelli *et al.*, *GEANT4: A simulation toolkit*, Nucl. Instr. Methods A**506** (2003), 250.

[13] P. Pralavorio, *Study of EM Calo response with minimum bias events*, Presentation at the LARG Week EM Calibration Meeting, Dec. 2006.

[14] W.E. Cleland and E.G. Stern, *Signal processing considerations for liquid ionization calorimeters in a high rate environment*, Nucl. Inst. Meth. A **338** (1994) 467.

[15] F. Hubaut *et al.*, *Study of the EM barrel module 0 with muons*, ATL-LARG-2001-017.

[16] P.-S. Mangeard, *Optimizing LAr Muon Cluster Reconstruction and Selection*, presentation at LARG Week BP3C Analysis Meeting, Dec. 2006.

[17] B. Resende, *Cosmic muons reconstruction : OFC Iter - 29 sample OFC*, presentation at LARG Week BP3C Analysis Meeting, Dec. 2006.

[18] https://uimon.cern.ch/twiki/bin/view/Atlas/MBTSInfo

[19] C. Buttar, *Minimum-bias in the early days: their selection and their use*, presentation at Trigger and Physics Week Plenary meeting, June 2006.

C. Buttar, *Minimum bias at 900 GeV*, presentation at MinBias Working Group Meeting, June 2006.

R. Kwee, *Triggering Minimum Bias events*, presentation at MinBias Working Group Meeting, Aug. 2006.

[20] B. Aubert *et al.*, *Construction, assembly and tests of the ATLAS electromagnetic barrel calorimeter*, Nucl. Instr. Methods A**558** (2006), 388.

Appendix 1: Error computation

Above the noise, the distribution of the energy deposited by minimum bias events in each calorimeter cell is exponentially decaying, with a mean value (μ) and a dispersion *RMS*. Applying the central limit theorem, if the occupancy *Occ*, i.e. the number of time that the cell is hit with an energy deposit 5σ above the noise, is high enough (typically greater than 100), the accumulated energy is gaussian with a mean value $E = Occ \times \mu$ and a variance $\sigma^2 = Occ \times RMS^2$. The accumulated energy in N neighbouring cells, with similar occupancy, is therefore:

$$E_N = N \cdot Occ \times \mu \pm RMS\sqrt{(N \times Occ)} \tag{3}$$

In the present note, we are considering the ratio R of the energies deposited at the same η region in two different ϕ zones, respectively with N_1 and N_2 cells. The error on this ratio can be expressed in the following way:

$$\frac{\Delta R}{R} \propto \frac{1}{\sqrt{Occ}} \left(\frac{1}{N_1^2} + \frac{1}{N_2^2} \right)^{\frac{1}{2}} \tag{4}$$

More particularly, if $N_1 = N_2 = N$ as in the case of two hemispheres:

$$\frac{\Delta R}{R} \propto \frac{\sqrt{2}}{N} \frac{1}{\sqrt{Occ}} \tag{5}$$

These formulae are used to extrapolate our results to an increased statistics and other sizes $\Delta\eta \times \Delta\phi$ of problematic regions, as needed for example for Figure 11.